

## Electron Transfer in Dye-Sensitized Nanocrystalline TiO<sub>2</sub> Solar Cell

M. Malekshahi Byranvand\*, A. Nemati Kharat, A. R. Badii

*School of Chemistry, University College of Science, University of Tehran, Tehran, Iran.*

### *Article history:*

Received 3/2/2012

Accepted 24/5/2011

Published online 1/6/2012

### *Keywords:*

Dye-Sensitized Solar Cells (DSSC)  
Electron transport  
Nanostructured TiO<sub>2</sub>  
Electron lifetime  
Nanocrystal.

### *\*Corresponding author:*

E-mail address:

mahdi.malekshahi@gmail.com

Phone: 98 916 9563280

Fax: +98 21 6112499

### **Abstract**

The dye-sensitized solar cells (DSSC) have been regarded as one of the most promising new generation solar cells. Tremendous research efforts have been invested to improve the efficiency of solar energy conversion which is generally determined by the light harvesting efficiency, electron injection efficiency and undesirable electron lifetime. In this review, various characteristics of dye-sensitized nanostructured TiO<sub>2</sub> solar cells, such as working principle, electron transport and electron lifetime, were studied. The review avoids detailed mathematical and spectroscopic discussion, but rather tries to summarize the key conclusions relevant to materials design.

2012 JNS All rights reserved

### **1. Introduction**

About 20 years ago, Grätzel and O'Regan published an article in Nature [1] that described a remarkably efficient photochemical solar cell based on the dye sensitization of mesoporous nanocrystalline titanium dioxide films. This new type of solar cell technology offered the promise of achieving moderate efficiency devices at ultra-low costs. In traditional photovoltaic cells, the

semiconductor functions to simultaneously (1) absorb visible light and (2) mediate electrons [2]. In contrast, DSSC are not limited by the light harvesting ability of the semiconductor; in fact, most are optically transparent. The sensitization of these semiconductors to visible light involves interfacial electron transfer following selective excitation of a surface-bound molecular chromophore [3]. Such a photoinduced charge-

separation process is a key step for solar energy conversion. Commonly studied chromophores, which will be referred to as dyes or sensitizers, include organic molecules and transition metal coordination compounds [4]. A schematic representation of a typical DSSC is illustrated in Fig.1 [5]. In the most common and most efficient devices to date, light is absorbed by a ruthenium complex, such as  $(\text{Bu}_4\text{N})_2[\text{Ru}(4,4'\text{-dicarboxy-2,2'\text{-bipyridine})}_2(\text{NCS})_2]$  [6], that is bound to a metal oxide photoanode via carboxylate moieties. Sensitized electrodes with  $\text{TiO}_2$  show both ultrafast electron injection rates and slow recombination rates required to make efficient DSSCs [7]. The 50 - 70 % porosity allows facile diffusion of redox mediators within the film so they can react with surface-bound sensitizers for efficient regeneration of the photoanode. The band gap of  $\text{TiO}_2$  is 3.2 eV, corresponding to light absorption below 380 nm. Because of its optical transparency to visible light, sensitization with molecular chromophores is required to harvest sunlight. Following light absorption, the exciton is split across the dye/nanoparticle interface in femtoseconds to picoseconds. The injected electron diffuses through the sintered particle network to be collected at the TCO, while the oxidized dye is reduced by a redox shuttle,  $\text{I}^-/\text{I}_3^-$ , dissolved in a solution that both permeates the porous photoelectrode and contacts the circuit-completing dark electrode (typically, platinized TCO) [8].

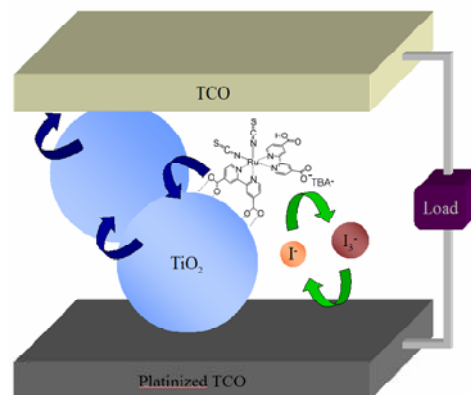


**Fig.1.** Schematic of a DSSC.

In this paper, we review our recent work on the kinetics and mechanism of electron injection in dye-sensitized nanocrystalline semiconductors. Section 2 of this paper provides a brief description of the working principle of dye sensitized solar cell. Sections 3 and 4 discuss the evidence and models that are invoked to explain the electron transport and the electron dynamic mechanisms.

## 2. Working principle DSSC

The details of the operating principles of the dye-sensitized solar cell are given in Fig.2 [9]. The photoexcitation of the metal-to-ligand charge transfer (MLCT) of the adsorbed sensitizer (Eq. 1) leads to injection of electrons into the conduction band of the oxide (Eq. 2). The oxidized dye is subsequently reduced by electron donation from an electrolyte containing the iodide/triiodide redox system (Eq. 3). The injected electron flows through the semiconductor network to arrive at the back contact and then through the external load to the counter electrode. At the counter electrode, reduction of triiodide in turn regenerates iodide (Eq. 4), which completes the circuit. With a closed external circuit and under illumination, the device then constitutes a photovoltaic energy conversion system, which is regenerative and stable. However, there are undesirable reactions, which are that the

injected electrons may recombine either with oxidized sensitizer (Eq. 5) or with the oxidized redox couple at the  $\text{TiO}_2$  surface (Eq. 6), resulting in losses in the cell efficiency[5].

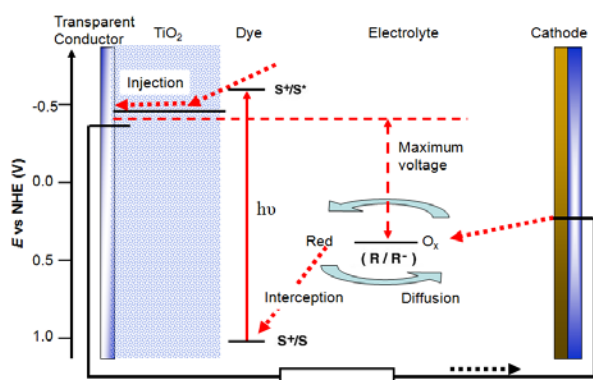
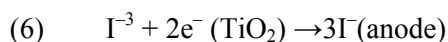
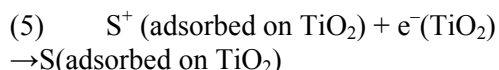
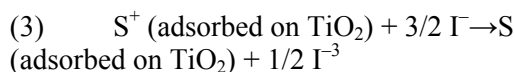
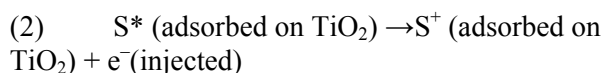
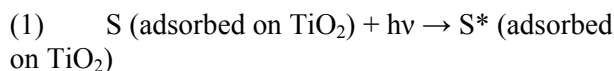


**Fig. 2.** Operating principles of DSSC

At the heart of the system is a mesoporous oxide layer composed of nanometer-sized particles, which have been sintered together to allow electronic conduction to take place. The material of choice has been  $\text{TiO}_2$  (anatase) although alternative wide band gap oxides such as  $\text{ZnO}$ ,  $\text{SnO}_2$  and  $\text{Nb}_2\text{O}_5$  have also been investigated [10]. Attached to the surface of the nanocrystalline film is a monolayer of a sensitizer. The high surface area of

the mesoporous metal oxide film is critical to efficient device performance as it allows strong absorption of solar irradiation to be achieved by only a monolayer of adsorbed sensitizer [11]. The use of a dye monolayer avoids any requirement for excited state (or “exciton”) diffusion to the dye/metal oxide interface. It also avoids the acceleration in non-radiative excited state decay to ground state that is often associated with thicker molecular films. The use of a mesoporous film results in a dramatic enhancement of the interfacial surface area by more than 1000-fold for a 10mm thick film. This leads to high visible light absorbance from the monolayer of adsorbed dye [12].

### 3. Electron Transport through

The most extensively applied and successful material by far is the high bandgap semiconductor  $\text{TiO}_2$  (bandgap: 3.2 eV). The often translucent nanocrystalline layers consist of interconnected colloidal particles in the size range of 15–30nm with a layer thickness typically between 5 and 15  $\mu\text{m}$  [13]. The best photovoltaic performances have been obtained using layers with enhanced haze and by application of a  $\text{TiCl}_4$  posttreatment [14]. Enhanced haze is achieved by introduction of scattering centers (large  $\text{TiO}_2$  particles) inside or on top of the film with the smaller particles [15]. The colloidal  $\text{TiO}_2$  materials are prepared by a hydrothermal sol-gel method in acidic or basic aqueous media and the layers are generally applied by industrially relevant processes such as screen-printing. For a quantitative removal of organic additives (binders and dispersants) after printing, processing temperatures between 450 °C and 550 °C are typically required during the annealing of the films. An SEM image of the top view of a typical  $\text{TiO}_2$  film is shown here in Fig. 3 [16].

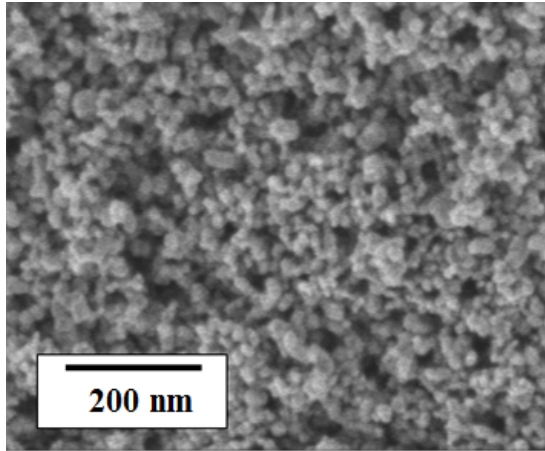


**Fig. 3.** SEM micrograph of a nanocrystalline TiO<sub>2</sub> film.

The mechanism for electron transport through mesoporous TiO<sub>2</sub> is still a hotly debated topic. Deducing the exact mechanism through experimental and theoretical investigations is

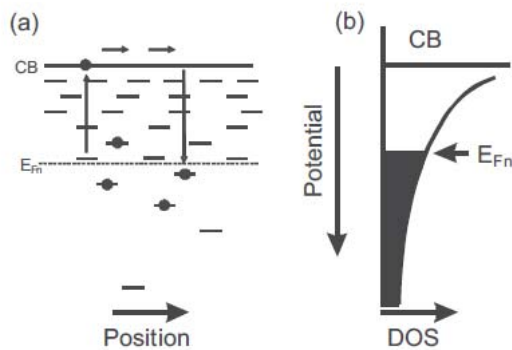


**Fig. 4.** **a)** Schematic illustration of the trap distribution and the multiple trapping–detrapping process occurring in mesoporous titania. **b)** Illustration of the density-of-states (DOS) distribution in solid films.

In its briefest form, the occupation of sub band gap states at energy  $E_A$  is given by the Fermi-Dirac distribution function, and the density of carriers at this energy is,  $n_A = N_A F(E_A)$ , where  $N_A$  is the total number of available sites at this energy (Eq. 7).

complicated, partly because of the apparent inability to systematically vary individual parameters without influencing others. Two undisputed observations are that the electron mobility in mesoporous TiO<sub>2</sub> is many orders of magnitude lower than that in single crystals, and that there exist subbandgap states in the TiO<sub>2</sub> that influence the transport, though the distribution and location of these states is still under debate. There is much experimental and theoretical evidence that supports the notion that the electron transport is governed by a detrapping of electrons from these sub-bandgap states, deep in the tail of the density-of-states (DOS), to the conduction band (CB), [17-19] consistent with the multiple-trapping (MT) model for charge transport is shown in Fig. 4 [20,21].

$$(7) \quad F(E_A + E_{Fn}) = \frac{1}{1 + e^{(E_A - E_{Fn})/k_b T}}$$

If we consider that electrons can only be transported via the conduction band, then we need to consider how the density of electrons in the conduction band ( $n_{CB}$ ) varies with the position of the quasi-Fermi level for electrons ( $E_{Fn}$ ). Specifically, [22] with the conductivity of the film being proportional to  $n_{CB}$  (Eq. 8).

$$(8) \quad n_{CB} = N_{CB} e^{(E_{Fn} - E_{CB})/k_b T}$$

The average electron mobility then depends upon the probability of the electrons being in the conduction band, and thus increases as the quasi-Fermi level for electrons approaches the conduction band energy. Knowledge of the exact location of the “transport-limiting” traps is likely

to be critically important in order to fully understand the transport mechanism in this material. The location of the traps has been thought to be in the bulk of the crystals, [18] at the interparticle “grain boundaries”, [23] and on the surface of the nanoparticles [24,25].

#### 4. Electron dynamic in DSSC

In order to understand and advance DSSC technology, the kinetics and dynamics of charge movement have been examined in detail by many researchers, both experimentally and via computational modeling. The transfer of electrons and holes across several, often non-ideal and ill defined, heterogeneous interfaces is exceptionally complex. As such, the kinetics is sensitive to many subtle factors such as excitation wavelength and dye loading conditions [26, 27]. Since the kinetics are complicated and don't always conform to a simple rate law, rate constants aren't strictly meaningful. Herein we will follow the convention of reporting half-life times, Table 1, in order to appreciate the different time scales of the relevant processes that span nine orders of magnitude.

For each time constant, the value shown in Fig.6 is the most current literature datum measured on a standard cell under operating conditions, preferably at the maximum power point ( $\approx 700$  mV)[28-33]. In order to relate these processes to PV performance, the charge dynamics are best viewed on a modified energy level diagram, Fig. 5.

**Table 1.** Kinetic processes in DSSC [28].

Process	Half-life (second)
Injection	150 ps
Relaxation	12 ns
Regeneration	1 $\mu$ s
Recombination	3 $\mu$ s
Charge Transport	100 $\mu$ s
Charge Interception	1 ms

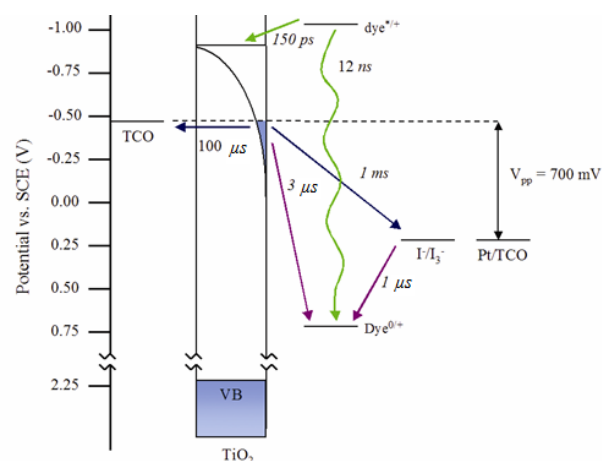


**Fig. 5.** Kinetic processes in DSSC [28].

The convenience of reporting half times of reaction rates may result in the misconception that there is considerable room for improvement by minimizing kinetic redundancy. For example, it appears that charge injection is almost 100 times faster than the competing process, relaxation of the excited state. If this were the case, then  $V_{OC}$  could be substantially enhanced by shifting the conduction band edge of  $TiO_2$  negative without loss of charge collection efficiency. That this is not the case (or at least not entirely) is due to the dispersive kinetics of charge injection. In fact, studies of competing processes have shown that in its most efficient

configuration a DSSC has comparatively little kinetic redundancy. This point may be visualized in Fig.6, in which order-of-magnitude estimates of area normalized rates at the maximum power point are taken from literature and presented as Gaussian curves on a logarithmic time scale [29-34].

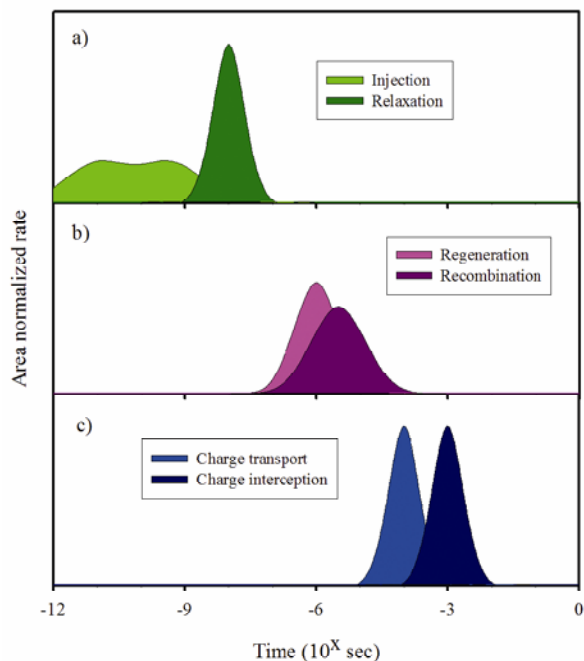


**Fig. 6.** Area normalized rates from literature show charge dynamics in direct kinetic competition at the maximum power point [28].

As state-of-the-art DSSCs have been optimized for maximum voltage while retaining near unity absorbed photon-to-current efficiency, dramatically new versions of the key components are warranted to advance the field. These could include new super chromophores that can collect light 10 to 100 times more efficiently than existing chromophores, new shuttles that can regenerate dyes at low driving force yet exhibit slow interception of injected charges, or new photoelectrode architectures [28].

## 5. Charge recombination

Charge recombination between dye cations and photoinjected electrons occurs non-exponentially over  $\mu\text{s}$ – $\text{ms}$  time scales. The wide range of time scales is usually attributed to the trapping of electrons by localized states on the  $\text{TiO}_2$  surface [35-37]. Nanocrystalline materials, possessing a high surface area, have a high density of such intra-band-gap trap states [38]. The distribution of trap energies results in the distribution of electron de-trapping times leading to dispersive transport. Experiments reveal strong sensitivity of the recombination rate to the occupancy of trap levels, which can be controlled by changing the intensity of the light source or the surrounding electrolyte composition, or by applying the external bias [35, 39]. Experiments also show that by modifying the dye structure one can switch between electron transport-limited dispersive recombination dynamics and interfacial electron transfer-limited exponential recombination dynamics [40].

## 6. Conclusion

Dye sensitized solar cells are photoelectrochemical solar devices, currently subject of intense research in the framework of renewable energies as a low-cost photovoltaic device. we have reviewed our recent theoretical work on the kinetics and mechanism of electron injection and charge recombination in dye-sensitized nanocrystalline semiconductors. This review has hopefully given the reader some insights into the parameters determining the efficiencies of electron injection and dye regeneration in dye sensitized photoelectrochemical solar cells.

### Acknowledgment

The financial support of this work by Research Council of University of Tehran.

### References

- [1] B. O'Regan, M. Gratzel, *Nat.* 353.(1991) 737.
- [2] D. Chapin, C. Fuller, G. Pearson, *J. Appl. Phys.* 25 (1954) 676.
- [3] O'Regan B. et al. *Adv. Mater.* 12 (2000). 7.
- [4] Cahen D. et al. *J. Phys. Chem. B.* 104 (2000) 2053.
- [5] Md. K. Nazeeruddin, S.M. Zakeeruddin, J.-J. Lagref, P. Liska, P. Comte, C. Barolo, G. Viscardi, K. Schenk, M. Graetzel, *Coord. Chem. Rev.* 248 (2004) 1317.
- [6] Nazeeruddin, M. K. Zakeeruddin, S. M. Humphry-Baker, R. Jirousek, M. Liska, P. Vlachopoulos, N. Shklover, V. Fischer, C. H. Gratzel, *M. Inorg. Chem.* 38 (1999) 6298.
- [7] Ferber, J. et al. *Sol. Energ. Mat. Sol. Cel.* 53 (1998) 29.
- [8] Srikanth K. et al. *Sol. Energ. Mat.Sol. Cel.* 65 (2001) 171.
- [9] Levine, I. N. 1978, McGraw-Hill, ISBN 0-07-066388-2.
- [10] Hagfeldt A. Grätzel M. *Chem. Rev.* 95 (1995) 49.
- [11] M. M. Malekshahi Byranvand, M.H. Bazargan, A. Nemati Kharat, *Digest Journal of Nano. mate. B.* 5 (2010) 587
- [12] M.H. Bazargan, M. M. Malekshahi Byranvand, A. Nemati Kharat, *Chalcogenide Lett.* 7 (2010) 515.
- [13] C. J. Barb' e, F. Arendse, P. Comte, et al. 80 (1997) 3157.
- [14] P. M. Sommeling, B. C. O'Regan, R. R. Haswell, et al, *Journal of Physical Chemistry B.* 110 (2006) 19191.
- [15] S. Ito, S. M. Zakeeruddin, R. Humphry-Baker, et al. *Advanced Materials.* 18 (2006) 1202.
- [16] K. Sayama, H. Sugihara, and H. Arakawa, *Chem. Mater.* 10 (1998). 3825.
- [17] J. Nelson, *Phys. Rev. B.* 59 (1999) 374.
- [18] J. Bisquert, *J. Phys. Chem. B.* 108 (2004) 2323.
- [19] L. Dloczik, O. Ileperume, I. Laueremann, L. M. Peter, E. A. Ponomarev, G. Redmond, N. J. Shaw, I. Uhlendorf, *J. Phys. Chem. B.* 101 (1997) 10.
- [20] J. Orenstein, M. Kastner, *Phys. Rev. Lett.* 46 (1981) 1421.
- [21] T. Tiedje, A. Rose, *Solid State Commun.* 37 (1981) 49.
- [22] J. Bisquert, V. S. Vikhrenko, *J. Phys. Chem. B.*, 108(2004) 2313.
- [23] M. Adachi, Y. Murata, J. Takao, J. Jiu, M. Sakamoto, F. Wang, *J. Am. Chem. Soc.* 126 (2004) 14.
- [24] G. Franco, J. Gehring, L. M. Peter, E. A. Ponomarev, I. Uhlendorf, *J. Phys. Chem. B.* 103 (1999) 692.
- [25] G. Schlichthörl, N. G. Park, A. J. Frank, J. *Phys. Chem. B.* 103 (1999) 782.
- [26] Benko, G. Kallioinen, J. Korppi-Tommola, J. E. I. Yartsev, A. P. Sundstrom, V. *Journal of the Am. Chem. Soc.* 124 (2002) 489.
- [27] Wenger, B. Gratzel, M. Moser, J. E. *Journal of the Am. Chem. Soc.* 127 (2005) 12150.
- [28] A. B. F. Martinson, Thomas W. Hamann, Michael J. Pellin, Joseph T. Hupp. *Chem. Eur. J.* 14 (2008) 4458.
- [29] Haque, S. A. Palomares, E. Cho, B. M. Green, A. N. M. Hirata, N. Klug, D. R. Durrant, J. R. *Journal of the Am. Chem. Soc.* 127 (2005) 3456.
- [30] Kroeze, J. E. Hirata, N. Koops, S. Nazeeruddin, M. K. Schmidt-Mende, L. Gratzel, M. Durrant, J. R. *Journal of the Am. Chem. Soc.* 128 (2006) 16376.

- [31] Clifford, J. N. Palomares, E. Nazeeruddin, M. K. Gratzel, M. Durrant, J. R. J. Phys. Chem. C. 111 (2007) 6561.
- [32] Palomares, E. Clifford, J. N. Haque, S. A. Lutz, T. Durrant, J. R. J. Am. Chem. Soc. 125 (2003) 475.
- [33] O'Regan, B. C.; Bakker, K.; Kroeze, J.; Smit, H.; Sommeling, P.; Durrant, J. R., Journal of Physical Chemistry B 2006, 110, (34), 17155-17160.
- [34] Durrant, J. R.; Haque, S. A.; Palomares, E., Coordination Chemistry Reviews 2004, 248, (13-14), 1247-1257.
- [35] S.A. Haque, Y. Tachibana, R.L. Willis, J.E. Moser, M. Grätzel, D.R. Klug, J.R. Durrant, J. Phys. Chem. B 104 (2000) 538.
- [36] S.Y. Huang, G. Schlichthörl, A.J. Nozik, M. Grätzel, A.J. Frank, J. Phys. Chem. B. 101 (1997) 2576.
- [37] A.V. Barzykin, M. Tachiya, J. Phys. Chem. B. 106 (2002) 4356.
- [38] A. Hagfeldt, M. Grätzel, Chem. Rev. 95 (1995) 49.
- [39] S.A. Haque, Y. Tachibana, D.R. Klug, J.R. Durrant, J. Phys. Chem. B. 102 (1998) 1745.
- [40] J.N. Clifford, G. Yahioglu, L.R. Milgrom, J.R. Durrant, Chem. Commun. (2002) 1260.